An engineered substance P variant for receptor-mediated delivery of synthetic antibodies into tumor cells

Shahir S. Rizk[a], Anna Luchniak[a,b], Serdar Uysal[a], Crista M. Brawley[a], Ronald S. Rock[a], and Anthony A. Kossiakoff[a,1]

[a]Department of Biochemistry and Molecular Biology, University of Chicago, 929 E. 57th Street, Chicago, IL 60637; and [b]Department of Biology and Earth Sciences, Jagiellonian University, ul. R. Ingardena 6, 30-060 Cracow, Poland

Communicated by James A. Wells, University of California, San Francisco, CA, May 11, 2009 (received for review January 15, 2009)

We have developed and tested a robust delivery method for the transport of proteins to the cytoplasm of mammalian cells without compromising the integrity of the cell membrane. This receptor-mediated delivery (RMD) technology utilizes a variant of substance P (SP), a neuropeptide that is rapidly internalized upon interaction with the neurokinin-1 receptor (NK1R). Cargos in the form of synthetic antibody fragments (sABs) were conjugated to the engineered SP variant (SPv) and efficiently internalized by NK1R-expressing cells. The sABs used here were generated to bind specific conformational forms of actin. The internalized proteins appear to escape the endosome and retain their binding activity within the cells as demonstrated by co-localization with the actin cytoskeleton. Further, since the NK1R is over-expressed in many cancers, SPv-mediated delivery provides a highly specific method for therapeutic utilization of affinity reagents targeting intracellular processes in diseased tissue.

actin | drug delivery | synthetic antibody fragment

Directed delivery of bioactive reagents into cells is one of the most intensely pursued objectives in biomedical research, yet few major breakthroughs have materialized that can be broadly applied in both laboratory research and therapeutic applications. Transfection reagents (1–3) as well as cell-penetrating peptides (4–7) lack cell-type specificity, and in many cases are associated with heavy toxicity (8), restricting the successful utilization of such reagents in vivo. In contrast, receptor-mediated delivery (RMD) systems (9–11) are conceptually simple and potentially very powerful. By attaching a biomolecular cargo to a natural ligand, receptor-mediated internalization serves as an extremely efficient and selective pathway for delivery of a wide variety of bioactive entities without compromising the integrity of the cell membrane (Fig. 1). Previously described RMD methods rely on cargo attachment to hormones (12) or monoclonal antibodies that recognize a cell-surface receptor (13). However, these large protein ligands can be difficult to isolate or modify in a specific manner.

Here we present a delivery method based on substance P (SP), an 11 amino acid neuropeptide that is rapidly internalized through specific interaction with the neurokinin-1 receptor (NK1R) (14–16). We have engineered a variant of SP (SPv) that enables the specific delivery of proteins to NK1R-expressing cells. Unlike larger ligands, SPv is easily chemically synthesized, allowing the incorporation of various reactive groups to facilitate coupling to myriad biomolecular cargos. Importantly, the NK1R is highly over-expressed in several aggressive tumors (17, 18), particularly astrocytomas and glioblastomas (19, 20), where the level of expression is correlated with the degree of malignancy (21). Consequently, an RMD system using SPv could provide a high level of specificity for the targeting of tumor tissue, with little toxicity for noncancerous cells.

To evaluate the efficacy of the SPv-NK1R delivery system, we used a set of synthetic antibody fragments (sABs) selected from phage display libraries to bind various forms of actin. sABs resemble the Fab fragment of an antibody, consisting of a 55-kDa heterodimer of the heavy and light chain variable fragments, forming 1 antigen binding site that can be engineered to bind a specific target protein (22–24). A subset of these sABs can induce changes to actin structure or organization in vitro. We demonstrate that sABs conjugated to SPv are rapidly internalized only by cells expressing the NK1R. The internalized sABs appear to escape the endosomes and retain their in vitro properties by altering actin organization within the cytoplasm. Additionally, we take advantage of the over-expression of the NK1R in the human glioblastoma cell line U87 (20) to confirm the utility of SPv as a highly specific delivery vehicle that differentiates between tumor and non-tumor cells. Our findings suggest that the SPv-NK1R system could be used in an array of applications, from live cell imaging, mapping signaling pathways, as well as mediating delivery of therapeutic affinity reagents to disrupt intracellular components within tumor cells.

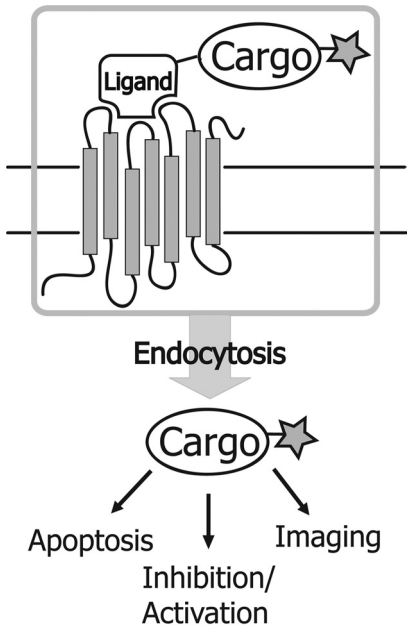

Fig. 1. Receptor-mediated delivery. A fluorescently-labeled cargo is attached to a natural ligand. Upon binding to the receptor, the cargo is internalized where it can carry out the desired function.

Author contributions: S.S.R. and A.A.K. designed research; S.S.R. and A.L. performed research; S.U. and C.M.B. contributed new reagents/analytic tools; S.S.R., A.L., C.M.B., and R.S.R. analyzed data; and S.S.R. and A.A.K. wrote the paper.

The authors declare no conflict of interest.

[1]To whom correspondence should be addressed. E-mail: koss@bsd.uchicago.edu.

This article contains supporting information online at www.pnas.org/cgi/content/full/0904907106/DCSupplemental.

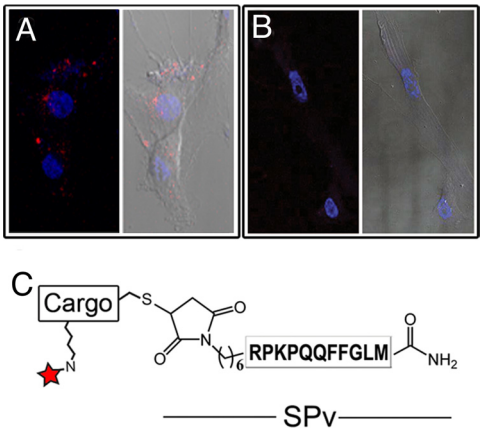

Fig. 2. Specific delivery of cargo to tumor cells by SPv. (*A*) U87 glioblastoma incubated with Alexa555-labeled SP for 2 h followed by fixing and nuclear staining (blue) show internalization of the peptide (red). (*B*) Normal human astrocytes show no detectable internalization of the peptide. (*C*) Conjugation of SPv to protein cargo. SPv is synthesized to contain the amino acid sequence of SP (boxed) in addition to an N-terminal maleimide for attachment of protein cargo via a surface cysteine residue. An amine reactive fluorophore (star) is attached to the cargo via surface lysines.

Results

Engineering a Delivery Vehicle Based on Substance P. Substance P (SP) is an 11 amino acid neuropeptide that is specifically internalized through binding to the NK1R, a member of the tachykinin G-coupled receptor family (14–16). The NK1R is highly overexpressed in brain tumor cells (19) compared with normal astrocytes. As a result, U87 glioblastoma cells readily internalize fluorescently-labeled SP (Fig. 2*A*), while internalization is undetectable in normal human astrocytes (NHA) (Fig. 2*B*). Additionally, western blot analysis of the NK1R expression confirms significant levels of receptor expression in U87 (19), whereas the receptor is undetectable in NHA (Fig. S1).

We used the selectivity of SP internalization by NK1R-expressing cells to engineer a specific vehicle for the delivery of protein cargo. A useful feature of SP is that only its C-terminal 7 amino acids are essential for binding to the NK1R and subsequent internalization (25), allowing incorporation of reactive groups for cargo attachment at the N terminus without affecting its function. Using standard *t*-Boc chemistry, we synthesized a variant of SP (SPv) with a "built-in" maleimide group at the N terminus. The maleimide moiety can be used to react with free cysteine residues under mild conditions to form a stable thioether bond (Fig. 2*C*), thus allowing attachment of any protein with free surface cysteines to SPv.

Specific Delivery of Actin-Binding sABs to NK1R-expressing Cells. To demonstrate the ability of SPv to deliver fully-functional protein cargo, we chose a set of synthetic antibody fragments (sABs) engineered by phage display selection to bind distinct conformational forms of actin filaments. Characterization of the in vitro actin-binding properties of 3 sABs (sAB-27, sAB-4, and sAB-19) shows that each sAB exhibits binding to the actin filaments. Electron microscopy imaging indicates that sAB-27 reconfigures the overall structure of actin by inducing filament bundling (Fig. 3*A*). In contrast, sAB-4 was shown to induce rapid severing of the actin filaments by total internal reflection fluorescence (TIRF) microscopy (Fig. 3*B*). Finally, sAB-19 binds to the end of the filaments without disrupting the overall actin structure (Fig. 3*C*). To conjugate the sABs to SPv, a cysteine mutation was introduced at position 121 of the heavy chain of each sAB. This position is solvent accessible and lies far from the antigen binding site, allowing conjugation to the SPv variant via the maleimide moiety without interfering with actin binding. Before attachment to SPv, each sAB was fluorescently labeled via surface lysines using an amine reactive fluorophore to facilitate visualization by confocal microscopy.

As the structure and location of intracellular actin are readily identifiable by phalloidin staining, the ability of SPv to deliver functional sABs can be rigorously tested by the ability of the internalized sABs to disrupt or localize with actin filaments. U87 cells were incubated for 2 h with 20 nM SPv conjugated to sAB-4, sAB-27, or sAB-19. The cells were then fixed, stained with phalloidin, and analyzed using confocal microscopy. A z-series of cells treated with the sAB-SPv conjugates confirms internalization and localization of the conjugate with actin filaments (Movie S1). Additional analysis of the confocal microscopy images indicates that the SPv-attached sABs internalized by U87 cells retain their in vitro properties by co-localization or reorganization of the cellular actin structure. Compared with untreated cells (Fig. 3*D*), SPv-mediated delivery of sAB-27 induces a conformational change to the actin filaments that stimulates bundling, drastically changing the overall shape of the actin filaments and, consequently, cell morphology (Fig. 3*E*). Similar results are obtained at very low concentrations (2 nM) of sAB-27-SPv. Cells treated with the sAB-4-SPv conjugate lack prominent stress fibers or actin-based protrusive structures (Fig. 3*F*), suggesting that sAB-4 induces severing of the filaments in the cytoplasm as observed in vitro (Fig. 3*B*). In contrast, the internalized sAB-19-SPv conjugate does not affect the overall structure of the actin filaments (Fig. 3*G*). In some cases, sAB-19 was found to localize to the base of filopodia (Fig. 3*G*, inset), presumably at the so-called pointed end of the actin filaments. A similar localization pattern was observed by immunostaining of fixed cells using fluorescently-labeled sAB-19 (Fig. S2). No internalization was observed after treatment of cells with up to 200 nM fluorescently-labeled sAB-4 alone (Fig. 3*H*). While in some cases the internalized sABs localize to peri-nuclear vesicles, the significant reorganization of intracellular actin indicates that a considerable fraction of the internalized sABs escapes the endosome in an active form.

Unlike U87 cells, HeLa cells lack significant amounts of the NK1 receptor. We therefore transfected HeLa cells with a plasmid coding for the NK1R, which then show the ability to internalize fluorescently-labeled SP alone (Fig. 3*I*) or SPv-conjugated sABs (Fig. 3*J* and *K*). As observed in U87 cells and in vitro, sAB-27 disrupts both the structure of the actin filaments and the overall cell morphology (Fig. 3*K*), while sAB-4 results in severing of actin filaments (Fig. 3*J*), compared to cells treated with SP only (Fig. 3*I*). The ability of the SPv-delivered sABs to affect the actin structure in transfected HeLa cells suggests that introduction of the NK1R is sufficient for the delivery of active cargo using SPv. Thus, this delivery technology has promise for a wide variety of transfectable mammalian cell lines.

The Effect of sAB-27 on Cell Viability. The interaction of actin filaments with many cellular components is essential to the normal function of cells. Thus, the actin-bundling activity of sAB-27, which significantly disrupts actin structure, would presumably have a drastic effect on the survival of cells. Therefore, we investigated the effect of sAB-27 on the viability of U87 glioblastoma cells following SPv-mediated delivery. U87 cells were treated with either 10 nM or 20 nM of SPv alone, sAB-27 alone, or the SPv-sAB-27 conjugate, and an MTS cell viability assay was carried out. Incubation of U87 cells with the SPv-sAB-27 conjugate showed a concentration-dependent decrease in cell viability compared with treatment with SPv or sAB-27 alone (Fig. 4*A*). A time-course of the viability of cells treated with the SPv-sAB-27 conjugate was carried out up to 48 h post-treatment. A drastic decrease in the viability of the gliobalstoma cells was observed within hours following treatment with

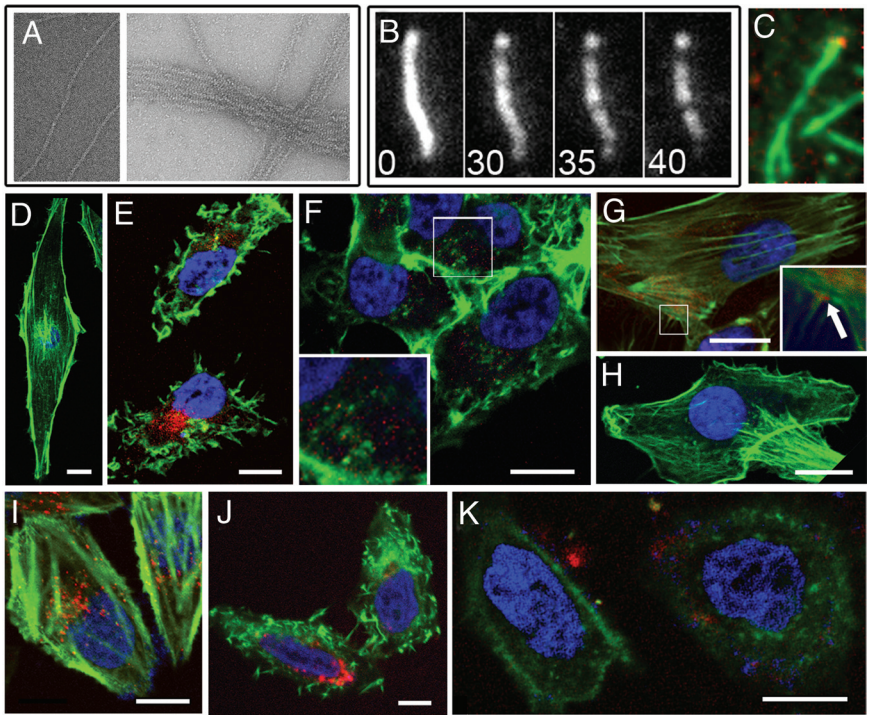

Fig. 3. Delivery of actin-binding sABs to cells expressing the NK1 receptor. (*A*) Electron micrographs of the bundling effect of sAB-27; left panel: actin only; right panel: actin in the presence of 6.4 μM sAB-27. (*B*) Severing of TMR-labeled actin filaments by sAB-4 viewed by TIRF microscopy. Numbers indicate time in seconds following addition of 0.5 μM sAB-4. (*C*) TIRF microscopy imaging of TMR-labeled actin filaments (green) in the presence of 0.25 μM cy5-labeled sAB-19 (red). (*D*) Phalloidin staining of untreated U87 glioblastoma cell. (*E*) The actin-bundling effect in U87 cells treated with 20 nM cy5-labeled sAB-27-SPv conjugate (red) followed by fixing and staining with TMR-phallodin (green). (*F*) U87 cells treated with 20 nM Alexa488-labeled sAB-4-SPv conjugate (red), followed by fixing and staining with TMR-phalloidin (green), inset: enlarged box showing severed actin filaments. (*G*) U87 cells treated with 20 nM Alexa488-labeled sAB-19-SPv conjugate (red) followed by fixing and staining with TMR-phalloidin (green); arrow in inset indicates an example of sAB-19 localizing to the base of filopodia. (*H*) U87 cells treated with 200 nM sAB-4 only exhibiting normal actin filaments. (*I–K*) HeLa cells transiently transfected with the NK1 receptor. (*I*) HeLa cells were treated with 100 nM SP-Alexa555 (red), then fixed and stained with FITC-phalloidin (green). (*J*) HeLa cells treated with 20 nM cy5-labeled sAB-27-SPv conjugate (red), followed by fixing and staining with TMR-phalloidin (green). (*K*) HeLa cells treated with 20 nM cy5-labeled sAB-4-SP conjugate (red) followed by staining with TMR-phallodin (green). (Scale bar, 10 μm.)

SPv-sAB-27(Fig. 4*B*), suggesting that the SPv-NK1R system may be useful in the treatment of several cancers.

Quantitative Analysis of SPv-mediated Internalization of sAB-27. To determine the efficiency of SPv-mediated delivery of proteins, U87 cells were incubated with increasing concentrations of a cy5-labeled SPv sAB-27 conjugate for 24 h in a 96-well plate. The cells were washed extensively with PBS and residual fluorescence was determined, reflecting the amount of internalized conjugate. The results show a correlation between the amount of conjugate added and the concentration of the internalized conjugate that fits a hyperbolic response (Fig. 5). Addition of as little as 2 pmol of the conjugate results in the retention of approximately 0.15 pmoles over roughly 5,000 cells in each well. Taking into account the average volume of U87 cells (500–1,000 μm^3), we estimate that the intracellular concentration of the conjugate is in the mid-micromolar range (30–60 μM). This indicates that even a

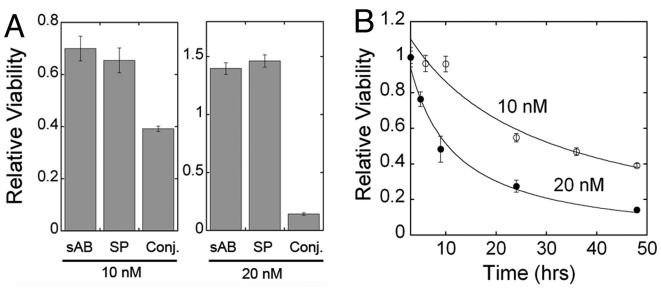

Fig. 4. Cell viability assay of U87 glioblastoma cells. (*A*) Forty-eight hour treatment with sAB27, SP or sAB-27-SPv conjugate; left panel, 10 nM; right panel, 20 nM. (B) Time course of inhibition of cell viability by the sAB27-SPv conjugate; open circles, 10 nM; closed circles, 20 nM.

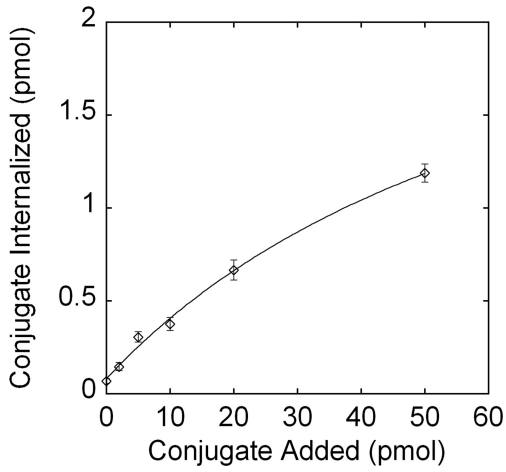

Fig. 5. Quantification of sAB-SPv conjugate internalization by U87 cells. Cells plated on a 96-well plate were treated with increasing amounts of sAB-27-SPv conjugate fluorescently labeled with cy5. After 24 h incubation, the cells were extensively washed, and the amount of the internalized conjugate was calculated from fluorescence values using a standard curve.

small fraction (≈1%) of the conjugate escaping the endosome would be comparable to the concentrations used for the in vitro studies, and would therefore, be sufficient to elicit a similar effect. It is important to note that the fit suggests an upper limit to the ability of U87 cells to internalize the SPv-conjugates with saturation at high concentrations of added conjugate. This apparent limit may be due to downregulation of the NK1R upon internalization of as a result of SPv uptake.

Discussion

We have developed an efficient and robust methodology that facilitates the delivery of protein cargos into the cytoplasm of live cells. The platform for our approach has been built such that it can be ported to the research community and used "out of the box." The method utilizes the receptor-mediated internalization of SPv as an efficient transmembrane delivery vehicle, circumventing many of the problems associated with traditional transfection approaches, such as cytotoxicity. While ligand-induced receptor internalization is a ubiquitous mechanism of receptor regulation, the SP-NK1R system offers several distinct advantages over other systems. SP is a short peptide with subnanomolar affinity to the NK1R. Because only the C-terminal portion of SP is required for binding to the receptor, a wide variety of cargos can be linked to the N terminus.

A crucial feature of this RMD system is that enough of the SPv conjugates appear to readily escape the endosome without loss of function. We have tested other ligand-receptor systems that are efficiently internalized, but in many cases the cargo appears to remain trapped in the endosome and are thus biologically inactive. Although it has been suggested that SP is quickly degraded after internalization (16), it is not clear why SPv-conjugated cargos escape the endosomal machinery more efficiently than in other systems. It is possible that by linking cargo to SP the peptide is sufficiently modified in character that its fate is effectively altered. How and why this occurs is beyond the scope of this study. However, essentially all protein-based cargo that we have conjugated to SPv have been successfully delivered to the cytoplasm without loss of function. In complementary studies, we have determined that our engineered SPv can deliver a wide variety of bioactive cargo including nucleic acid-based molecules such as siRNA, shRNA, and DNA, as well as imagining agents and proteins up to at least 400 kDa. While the delivery of RNA/DNA molecules appears to be promising, further work is needed to rigorously profile their bioactivity in live cells.

Combining our SPv delivery technology with the ability to introduce functional sABs into live cells could be a transformative advancement for studying signaling pathways and other intracellular functions. In extensive studies, we have determined that phage display library-sorting protocols can be designed to produce high affinity sABs that recognize a specific protein surface, a particular conformational state or a multicomponent complex. These attributes, combined with the ability to fine-tune the affinity to the target, result in a class of "designer" affinity reagents that can be programmed to carry out a wide range of directed functions within the cell following internalization. Examples of this include the sABs engineered against different forms of actin described here. Importantly, we have observed that sABs retain their function within the cytoplasm for at least several days after internalization. Thus, sABs engineered for live cell imaging, or inhibition or activation of specific junctions in signaling pathways will have an extended functional lifetime in a live cell system.

Another notable feature of the system is its exquisite specificity for targeting certain types of cancer cells. We have shown that internalization of SPv is restricted to cells expressing the NK1R. This receptor is overexpressed in many types of tumors and primary cancers, including breast carcinomas, adenocarcinomas of the colon, astrocytomas, and glioblastomas (17). This ability to discriminate between cancer cells expressing the NK1R and normal cells suggests that receptor-mediated delivery using SPv as a Trojan Horse for bioactive cargo may have great therapeutic potential. Further, the specific delivery of sABs directed toward cytoplasmic targets within tumor cells potentially changes the paradigm for antibody-based therapies. These therapies may no longer be limited to the current extracellular targets. Thus, using sABs designed to inhibit intracellular signaling nodes, the possibility certainly exists for focusing future antibody therapies toward a much richer set of cancer targets.

Methods

Peptide Synthesis of SPv Variants. All protected amino acids and resin for peptide synthesis were purchased from Peptides International, solvents from Fisher, salts and buffers from Sigma Aldrich. SPv-maleimide synthesis was carried out manually by standard t-Boc methods using *p*-methyl-benzhydrylamine resin to produce a C-terminal amide after HF cleavage. 6-Maleimidohexanoic acid (Sigma) was used to introduce an N-terminal maleimide with a 6-carbon linker. An additional variant of SP was synthesized that lacks the maleimide moiety but includes a cysteine mutation at position 3 for attachment of thiol-reactive Alexa-555 and was used as a positive control for NK1 receptor-mediated internalization. The peptides were cleaved from the resin using HF and extracted in 50% acetonitrile plus 0.1% trifluoroacetic acid aqueous solution for lyophilization. The purity of the crude peptides was determined using an analytical C-18 reversed-phase column on a Shimatzu 10A-vp and their masses were confirmed by MALDI MS.

Fluorescence Labeling and SPv Conjugation to sABs. Actin-binding sABs were engineered by phage display and purified as described (22). Each sAB contained a C-terminal 6-his tag and a cysteine mutation at position Ala-121 of the heavy chain. The purified sABs were dialyzed into 50 mM sodium borate buffer, pH 7.4, for fluorescent conjugation. NHS-ester fluorophores (Cy3 or Cy5; GE Healthcare, Alexa-488 or Alexa-647; Invitrogen) were added to each sAB in a 5-fold excess from a 10 mM stock solution in DMSO. Reactions were carried out at room temperature for 1 h, followed by gel filtration using a PD-10 column (GE Healthcare) equilibrated with 20 mM Mops, 100 mM NaCl pH 6.9 to remove excess fluorophore. The fluorescently-labeled sABs were reacted with a 10-fold excess of SPv-maleimide from a 5 mM stock in DMSO. The reaction was carried out overnight at 4 °C in 20 mM Mops, 100 mM NaCl, pH 6.9, followed by gel filtration using a PD-10 column to remove excess SPv.

TIRF Microscopy. Images were collected with a custom-built total internal reflection fluorescence microscope. A 100×, 1.45 NA objective (Olympus) and an EMCCD camera (Ixon, Andor Technologies) were used (*SI Methods*).

Electron Microscopy. Electron Micrographs were obtained on a FEI Tecnai F30 transmission electron microscope (*SI Methods*).

Cell Lines, Western Blots, and Transfection. See *SI Methods*.

Confocal Microscopy. For each sample, 10^4 U87 cells were seeded on an 18 mm cover-slip in MEM with10% FBS overnight in a 12-well plate, then starved in MEM with 0.1% BSA for 3 h. The reagent (SPv-sAB conjugate, SP-Fluorophore, or sAB only) was filter-sterilized, diluted to the desired final concentration in MEM 0.1% BSA and added directly to the live cells in each well for 2 h. Untreated cells or cells treated with sAB only served as a negative control. Following incubation with each reagent, the cells were washed 3 times with PBS, fixed in 4% *p*-formaldehyde, permeablized in TBST and blocked with 10% normal goat serum for 1 h. Actin filaments were stained with FITC-phalloidin (Invitrogen, 1:250 dilution), or TMR-phalloidin (Sigma-Aldrich, 1:3,000 dilution) for 1 h at room temperature. Nuclei were stained with either DAPI (10 mg/mL) or Hoechst reagent (Invitrogen, 1:2,000) for 5 min at room temperature, and samples were mounted using ProLong Gold reagent (Invitrogen). Confocal microscopy images were collected using a Leica SP2 confocal microscope with FITC and Alexa-488 excited by a 488 nm laser, TMR and Cy3 by a 543 nm laser, and Alexa 574 and Cy5 by a 633 laser. Multicolored images were overlaid using the ImageJ software.

MTS proliferation assay. CellTiter 96 AQ_{ueous} assay (Promega) was used to determine cell viability (see *SI Methods*).

ACKNOWLEDGMENTS. We thank Dr. Labno and Dr. Bindokas for valuable assistance with confocal microscopy imaging. This work was supported by National Institutes of Health Grants F32DK080619-02 (to S.S.R.) and GM078450 (to R.S.R.) and National Cancer Institute Grant T32CA009594 (to C.B.).

1. Dalby B, et al. (2004) Advanced transfection with Lipofectamine 2000 reagent: primary neurons, siRNA, and high-throughput applications. *Methods* 33:95–103.
2. Jacobsen LB, Calvin SA, Colvin KE, Wright M (2004) FuGENE 6 Transfection Reagent: The gentle power. *Methods* 33:104–112.
3. Felgner PL, et al. (1987) Lipofection: A highly efficient, lipid-mediated DNA-transfection procedure. *Proc Natl Acad Sci USA* 84:7413–7417.
4. Stewart KM, Horton KL, Kelley SO (2008) Cell-penetrating peptides as delivery vehicles for biology and medicine. *Org Biomol Chem* 6:2242–2255.
5. Morris MC, Depollier J, Mery J, Heitz F, Divita G (2001) A peptide carrier for the delivery of biologically active proteins into mammalian cells. *Nat Biotechnol* 19:1173–1176.
6. Youn JI, et al. (2008) Enhanced delivery efficiency of recombinant adenovirus into tumor and mesenchymal stem cells by a novel PTD. *Cancer Gene Ther* 15:703–712.
7. Vives E, Brodin P, Lebleu B (1997) A truncated HIV-1 Tat protein basic domain rapidly translocates through the plasma membrane and accumulates in the cell nucleus. *J Biol Chem* 272:16010–16017.
8. Cardozo AK, et al. (2007) Cell-permeable peptides induce dose- and length-dependent cytotoxic effects. *Biochim Biophys Acta* 1768:2222–2234.
9. Vyas SP, Singh A, Sihorkar V (2001) Ligand-receptor-mediated drug delivery: An emerging paradigm in cellular drug targeting. *Crit Rev Ther Drug Carrier Syst* 18:1–76.
10. Gust TC, Zenke M (2002) Receptor-mediated gene delivery. *Scientific WorldJournal* 2:224–229.
11. Kamiyama H, Zhou G, Roizman B (2006) Herpes simplex virus 1 recombinant virions exhibiting the amino terminal fragment of urokinase-type plasminogen activator can enter cells via the cognate receptor. *Gene Ther* 13:621–629.
12. Tian P, et al. (1999) A novel receptor-targeted gene delivery system for cancer gene therapy. *Sci China C Life Sci* 42:216–224.
13. Pardridge WM (2007) shRNA and siRNA delivery to the brain. *Adv Drug Deliv Rev* 59:141–152.
14. Mantyh PW, et al. (1995) Rapid endocytosis of a G protein-coupled receptor: substance P evoked internalization of its receptor in the rat striatum in vivo. *Proc Natl Acad Sci USA* 92:2622–2626.
15. Mantyh PW, et al. (1997) Inhibition of hyperalgesia by ablation of lamina 1 spinal neurons expressing the substance P receptor. *Science* 278:275–279.
16. Garland AM, Grady EF, Payan DG, Vigna SR, Bunnett NW (1994) Agonist-induced internalization of the substance P (NK1) receptor expressed in epithelial cells *Biochem J* 303:177–186.
17. Hennig IM, Laissue JA, Horisberger U, Reubi JC (1995) Substance-P receptors in human primary neoplasms: Tumoral and vascular localization. *Int J Cancer* 61:786–792.
18. Singh D, et al. (2000) Increased expression of preprotachykinin-I and neurokinin receptors in human breast cancer cells: Implications for bone marrow metastasis. *Proc Natl Acad Sci USA* 97:388–393.
19. Palma C, Maggi CA (2000) The role of tachykinins via NK1 receptors in progression of human gliomas. *Life Sci* 67:985–1001.
20. Lai JP, Douglas SD, Wang YJ, Ho WZ (2005) Real-time reverse transcription-PCR quantitation of substance P receptor (NK-1R) mRNA. *Clin Diagn Lab Immunol* 12:537–541.
21. Yamaguchi K, Richardson MD, Bigner DD, Kwatra MM (2005) Signal transduction through substance P receptor in human glioblastoma cells: Roles for Src and PKC delta. *Cancer Chemother Pharmacol* 56:585–593.
22. Fellouse FA, et al. (2007) High-throughput generation of synthetic antibodies from highly functional minimalist phage-displayed libraries. *J Mol Biol* 373:924–940.
23. Ye JD, et al. (2008) Synthetic antibodies for specific recognition and crystallization of structured RNA. *Proc Natl Acad Sci USA* 105:82–87.
24. Sidhu SS, Koide S (2007) Phage display for engineering and analyzing protein interaction interfaces. *Curr Opin Struct Biol* 17:481–487.
25. Kumar GK, Prabhakar NR (2003) Tachykinins in the control of breathing by hypoxia: pre- and post-genomic era. *Respir Physiol Neurobiol* 135:145–154.
26. Pardee JD, Spudich JA (1982) Purification of muscle actin. *Methods Enzymol* 85:164–181.
27. Rock RS, Rief M, Mehta AD, Spudich JA (2000) In vitro assays of processive myosin motors. *Methods* 22:373–381.
28. Otterbein LR, Graceffa P, Dominguez R (2001) The crystal structure of uncomplexed actin in the ADP state. *Science* 293:708–711.